37.0 ADVANCED ENGINEERED COATINGS WITH EXTENDED DIE LIFE FOR TOOLING

Nelson Delfino de Campos Neto (Mines)
Faculty: Stephen Midson, Andras Korenyi-Both and Michael Kaufman (Mines)
Industrial Mentors: Paul Brancaleon (NADCA) and Rob Mayer (Queen City Forging Co.)

This project started in Fall 2018, is a five-year effort, and is supported by the Defense Logistics Agency and CAPES in Brazil. The research performed during this project will serve as the basis for a Ph.D. thesis for Nelson Delfino de Campos Neto.

37.1 Project Overview and Industrial Relevance

Die coatings produced by physical vapor deposition (PVD) started being used in the die casting industry in the 1990s, but at that time the coatings were relatively simple in nature and tended to be used only to minimize soldering of molten aluminum to core pins. Since then, die casters have developed more complex multi-layer coating architectures, and have also started to look at the use of coatings for "lube-free" applications. However, the factors that prevent the die cast aluminum alloys from sticking to the coatings are still not fully understood, precluding optimal coating compositions from being identified. In addition, die coating architectures need to be identified that will allow the coatings to last as long as the dies (~100,000 shots).

The PVD coatings help prevent aluminum die castings from soldering to the die surfaces, allowing the amount of lubricant that is applied to the die to be reduced or even eliminated. Minimizing the use of lubricants will reduce production costs arising from the purchase of the lubricants, the clean-up of effluents, help reduce cycle time, and provide an extension in die life, resulting in lower per-part costs. Reduced lubricant also leads to a significant improvement of the quality of die castings, allowing them to be used in higher performance applications. Cost optimization is important for part manufacturers, as die casting is normally the lowest cost approach for producing complex-shaped components from aluminum alloys.

37.2 Previous Work – Background and Previous Results

A prior project was performed at the Colorado School of Mines (Mines) by Wang [37.1-37.2], where a variety of PVD coatings were evaluated, finding that AlCrN had the best performance of those tested. The AlCrN coating was applied to a commercial die and a plant trial was conducted at Mercury Castings, where they were able to reduce the use of conventional organic lubricants by ~85% and significantly reduce cycle time. The goal of this follow-on project is to build on the research performed by Wang, and achieve the complete elimination of conventional lubricants for the die casting process.

During the first two years of the project, the main focus was on developing an improved aluminum adhesion test, based on the test described in previous reports [37.3-37.5]. Molten aluminum tests (MAT) were performed on bare H13 and five different AlCrN coatings using the new approach. Due to different behavior exhibited by the coatings in the MAT, coating characterization techniques were applied to better understand the composition, structure and performance of these coatings as described in a previous report [37.6]. Two other laboratory tests were used to test the resistance of a number of coatings to molten aluminum attack: (i) modified ejection test (MET), and (ii) rotating immersion tests (RIT), as previously reported [37.7]. In the third year of the project, the results from a successful controlled laboratory lube-free die casting trial performed using a Buhler 250-ton die casting machine at The Ohio State University (OSU) were presented in detail in a previous report [37.8], where over 200 lube-free die castings were achieved. For this report, the results from an industry die casting trial performed at Stellantis (Kokomo Die Casting Plant) will be presented in detail.

37.3 Recent Progress

37.3.1 Industry Die Casting Trial at Stellantis - Methodology

The industry die casting trial on coated core pins was performed at the Stellantis die casting plant in Kokomo, IN. As shown in **Figure 37.1**, these experiments involved core pins that experience severe conditions as they are located directly in-front of the gate in a die used to produce a large automotive casting. Since only the core pins were coated, this die run using conventional application of lubricant spray, and around 2,500 castings were produced using each set of coated core pins. Qualitative comparison and quantitative measurements were performed to identify the amount

of aluminum soldered to each PVD coating. The qualitative assessment was based on visual inspection of the core pins after/during each trial by Stellantis personnel. The quantitative analysis was performed in two ways: (i) the mass change on the core pins due to aluminum soldering, and (ii) by the fraction of surface area of the core pin that was covered with aluminum based on image analysis of macrographs taken using a Keyence microscope. Scanning electron microscopy (SEM) with energy dispersive spectroscopy (EDS) was performed on the surface of the core pins after the trials. EDS line scans coupled with macro SEM images helped identify the different soldering mechanisms happening on the core pin surfaces within its length. Higher magnification EDS maps of each mechanism were acquired.

37.3.2 Industry Die Casting Trial at Stellantis - Results

Table 37.1 shows the grade given by Stellantis personnel based on visual analysis of soldering resistance along with their comments. **Table 37.1** also shows the results for the mass change of core pins Si-DLC-polished, AlCrN/TiCN-polished, and Al_2O_3-draw. Very similar results were found for mass change on core pin 5205 in the range + 0.17 g to + 0.20 g. For core pins 5215 more discrepancy was found since the Si-DLC-polished pin had an increase in mass of + 0.28 g, while the AlCrN/TiCN-polished pin had a decrease in mass of – 0.17 g.

Figure 37.2 shows a more detailed 3D reconstruction of both sides of the cores acquired using a Keyence microscope for the nitrided-draw, Si-DLC-polished, AlCrN/TiCN-polished, and Al_2O_3-draw. Since the other core pins were destroyed during removal from the die, the 3D analysis of those cores were not possible. The nitrided-draw on **Figure 37.2(a)** shows similar distribution of soldering in the facing gate side (GS) and on the opposite gate side (OP), and brownish corrosion marks can also be seen in several areas. For the Si-DLC-polished on **Figure 37.2(b)**, core pin 5215 showed similar distribution of soldering in GS and OP, but core pin 5205 had a much more concentrated soldering in the GS side while a little more distributed on the OP side. Blue oxidation marks are present closer to the tip surrounded with some brownish corrosion marks. AlCrN/TiCN-polished coating on **Figure 37.2(c)** shows a more concentrated soldering on the GS side, and the OP for 5205 presented a small concentration of soldering in the center and border, while OP for 5215 had more dispersed soldering through its length, concentraded closer to the pin tip and inclined radial areas along its length. Different surface heights can be inferred from these images, showing what seems to indicate that the coating has been partially removed in several areas of the core pin, with more occurences closer to the tip. Al_2O_3-draw coating on **Figure 37.2(d)** showed concentrated gross soldering in the center of GS and several spots of gross soldering in the same area in the OP. Gross soldering was more continuous in the GS than it was in the OP side.

By using image analysis in the Keyence software, these images were used for the quantification of the percentage of surface area covered with aluminum for the GS and OP, and these results are also shown in **Table 37.1**. **Figure 37.3** shows a comparison between soldering on core pins 5205 and 5215 for the same side (GS vs GS and OP vs OP) with the same coating and finish for direct comparison of which core pins suffered more soldering. The same number of occurrences were found for each core pin, but some differences were found for each coating. The AlCrN/TiCN-polished presented more soldering on the 5205 core pin in both sides, while for the nitrided-draw had more soldering on the 5215. The Si-DLC presented more soldering on the GS of 5215, but the opposite for the 5205. Calculating the average soldering for 5205 results in 42 ± 12 %, while for 5215 is 43 ± 18 %. So no obvious trend could be found, but more variability of soldering could be seen for the 5215, meaning that this core pin can suffer more or less with soldering.

Figure 37.4 compares the soldering fraction on the GS vs OP for the same core pin. A higher number of occurrences were found for the GS (5) against the OP (2). The only two occurrences where the OP had more soldering were on core pin 5205 for the Si-DLC-polished and on the 5215 for the nitrided-draw, so no tendency based on core pin was found. But, a higher total fraction of surface covered with soldering was found for the core pin GS = 48 ± 14 % in comparison with the OP = 36 ± 15 % calculated for all coatings. For the GS, Si-DLC-polished coating showed the smallest amount of soldering for the 5205 pin, while for the OP the AlCrN/TiCN-polished coating had the smallest fraction of soldering on the 5215 pin.

Figure 37.5 compares the average of soldering for the different coatings. All the coatings had less soldering than the uncoated H13 with only a nitriding treatment. The Si-DLC-polished presented the least amount of soldering within the tested coatings. The Si-DLC-polished and the nitrided-draw showed more soldering in the 5215 core pin than in the 5205, the opposite happened for the AlCrN/TiCN. In general, the polished condition resulted in less soldering than in those with draw finish, what is in agreement with the qualitative results from the grading performed by Stellantis personnel. **Figure 37.6** compares the quantitative soldering results with the qualitative grade provided by Stellantis

personnel, and some agreement in the tendency on the plot could be found. Visual inspection is a qualitative method where results close to the average can be inspected, the discrepancy here was in attributing a better grade to Al_2O_3-draw than for the AlCrN/TiCN-polished, what is also understandable due to big spread on the AlCrN/TiCN results.

SEM analysis was performed for the surface of the core pin 5215 after the trials. **Figure 37.7(a)** shows an SEM BSE image for the Si-DLC-polished GS and **Figure 37.7(b)** for the OP, on the length of the core pin along with the EDS line scans. The combination of the BSE image and the EDS line scan and presented, and below is shown the proposed primary mechanism(s) of interaction at each position of the core pin along its length. As presented for the GS on **Figure 37.7(a)**, from left to right, the bigger diameter starts with a region were the coating is still pristine (OK), then it enters a region were coating erosion is the main mechanism (Erosion), and in the transition from the bigger to the smaller diameter the coating is conserved (OK). A huge portion of the center length of the core pin is covered with aluminum soldering, but also there is still coating on those areas with minor erosion (Soldering on Coating), then it enters into another region where the coating is preserved (OK). Close to the tip of the core pin it can be seen that erosion dominates combined with some minor soldering (Erosion + Soldering). At this point, most of the coating has been removed from the surface of the core pin. A very similar behavior can be seen for the OP side of the core pin, the main differences being the length along which each mechanism occurs. From left to right, the first region exhibits erosion, followed by a long length where the coating was preserved with minor erosion marks. As we move to the right, the differences are bigger, where there are changing mechanisms over small areas: first, soldering is observed on an eroded area where the coating has been removed (Erosion + Soldering) then, an area where some erosion happened but there is also soldering to the coating (Erosion + Coating Soldering), and finally followed by another area where the coating has been totally removed (Erosion). Closer to the tip of core pin it is similar to what was observed for GS: the coating has been removed by erosion and soldering happened, but it seems that more soldering has happened on this position for OP than for GS, and these differences are likely due to the GS being influenced by fast filling molten aluminum eroding the coating and also removing the soldering layers previously formed, while the OP side may be suffering from soldering and also dragging, or sheared lips, as previously proposed by Chen [37.9].

Figure 37.8 and **Figure 37.9** show more detailed analysis of each different mechanism for the Si-DLC-polished core pin GS and OP, respectively. **Figure 37.8(a)** and **Figure 37.9(a)** shows the region of the bigger diameter of the core pin where erosion was the main mechanism, as can be seen by the EDS map for Fe. The same eroded regions suffered with limited soldering as shown in the map for Al. **Figure 37.8(b)** shows the region of "soldering on coating" where a lot of Al can be seen in the EDS maps, but the coating is still present underneath the soldered layer as evidenced by the Si and C maps. Also, these results were combined with minor erosion indicated by the Fe maps, which could indicate the positions where the aluminum soldering occurred underneath the steel [37.10]. Interesting to note that in these same regions, a concentration of Mg and O can also be found, which suggests that Mg from the A380 alloy may be assisting coating oxidation and creating an easy path to the substrate, and similar results have been reported previously [37.11]. **Figure 37.8(c)** shows the transition from the soldered region in **Figure 37.8(b)** to the region where the coating was preserved (OK), some very limited erosion (Fe map), and some superficial rounded particles containing Mg and O found on the non-soldered side (right), which again suggests some influence Mg on this coating failure [37.11]. **Figure 37.8(d)** shows a region from the transition where the coating was preserved up to closer to the tip of the core pin where erosion + soldering prevailed, as can be seen in the EDS maps for Fe and Al in the right side without indication of coating elements (Si and C) present in that region. **Figure 37.9(b)** shows a coated region (OK) with very minor soldering (Al map) and minor erosion (Fe map) indicating a good preservation of the coating in those regions. **Figure 37.9(c)** shows an area with erosion and soldering happening on the same area as can be seen by the overlap of Fe and Al maps and Si and C absent from those regions. The Fe map also shows areas surrounding the soldered Al area. Interesting on this region is that the Mg and O maps lay exactly on the Al soldering map, and inside the area where the Al is lacking, the Mg is more concentrated. Since it is A380 alloy, the presence of Si particles would be expected on the soldered region but that is not observe in the EDS maps, which means that the soldering may be happening by the shear fracture of the casting soldered to the surface during ejection as proposed by Chen [37.9]. Finally, **Figure 37.9(d)** shows the erosion + soldering up to the rounded tip of the core pin. In the rounded region, the Si and C EDS maps show that the coating is still present there, surrounded by the Fe map indicating coating erosion, also the Mg and O maps surround the coated region and the eroded region, again indicating that the Mg from the A380 alloy may be the key element on the oxidation and failure of the Si-DLC coating, probably through oxidation as the O map follows the Mg maps [37.11].

37.4 Plans for Next Reporting Period

- Continue to evaluate the published literature to characterize wetting, PVD coatings, chemical interactions between liquid metals and ceramics, and brazing.
- Continue the in-plant die casting trials on a number of selected coatings.
- Characterization of the PVD coated samples using a range of techniques: electron microscopy, tribology, and surface analysis.
- Characterization of the soldered surfaces to understand solder and adhesion, interdiffusion, phase formation, and defects.

37.5 Acknowledgements

- This program is sponsored by the Defense Logistics Agency – Troop Support, Philadelphia, PA and the Defense Logistics Agency Information Operations, J68, Research & Development, Ft. Belvoir, VA.
- This study was financed in part by the Coordenação de Aperfeiçoamento de Pessoal de Nível Superior - Brasil (CAPES) - Finance Code 001. N.D. Campos Neto is thankful to CAPES Brazil for a scholarship from the program DOC-PLENO - Full Doctorate Abroad - Call No. 48/2017 - Selection 2018 process number 88881.175453/2018-01.

37.6 References

[37.1] B. Wang, An Investigation of the Adhesion Behavior of Aluminum on Various PVD Coatings Applied to H13 Tool Steel to Minimize or Eliminate Lubrication During High Pressure Die Casting, PhD thesis, CSM, 2016.

[37.2] B. Wang, G.R. Bourne, A.L. Korenyi-Both, A.K. Monroe, S.P. Midson, M.J. Kaufman. Method to evaluate the adhesion behavior of aluminum-based alloys on various materials and coatings for lube-free die casting. Journal of Materials Processing Technology, vol 237, pp 386-393, 2016.

[37.3] N. D. Campos Neto, A. Korenyi-Both, S. Midson, M. J. Kaufman. Advanced Engineered Coatings with Extended Die Life for Tooling. CANFSA Biannual Report, Project 37, March 25, 2019.

[37.4] N. D. Campos Neto, A. Korenyi-Both, S. Midson, M. J. Kaufman. Advanced Engineered Coatings with Extended Die Life for Tooling. CANFSA Biannual Report, Project 37, October 2, 2019.

[37.5] N. D. Campos Neto, A. Korenyi-Both, S. Midson, M. J. Kaufman. Advanced Engineered Coatings with Extended Die Life for Tooling. CANFSA Biannual Report, Project 37, April 7, 2020.

[37.6] N. D. Campos Neto, A. Korenyi-Both, S. Midson, M. J. Kaufman. Advanced Engineered Coatings with Extended Die Life for Tooling. CANFSA Biannual Report, Project 37, October 13, 2020.

[37.7] N. D. Campos Neto, A. Korenyi-Both, S. Midson, M. J. Kaufman. Advanced Engineered Coatings with Extended Die Life for Tooling. CANFSA Biannual Report, Project 37, April 6, 2021.

[37.8] N. D. Campos Neto, A. Korenyi-Both, S. Midson, M. J. Kaufman. Advanced Engineered Coatings with Extended Die Life for Tooling. CANFSA Biannual Report, Project 37, October 12, 2021.

[37.9] Z.W. Chen. Formation and progression of die soldering during high pressure die casting. Materials Science and Engineering A, 397, 356–369, 2005.

[37.10] Q. Han. Mechanism of die soldering during aluminum die casting. CHINA FOUNDRY Overseas Foundry, Vol.12, No.2, 2015.

[37.11] C. Vian. TECHNOLOGY FOR THE ADVANCEMENT OF DIE CASTING TOOLING. PhD thesis, Purdue University, 2021.

37.7 Figures and Tables

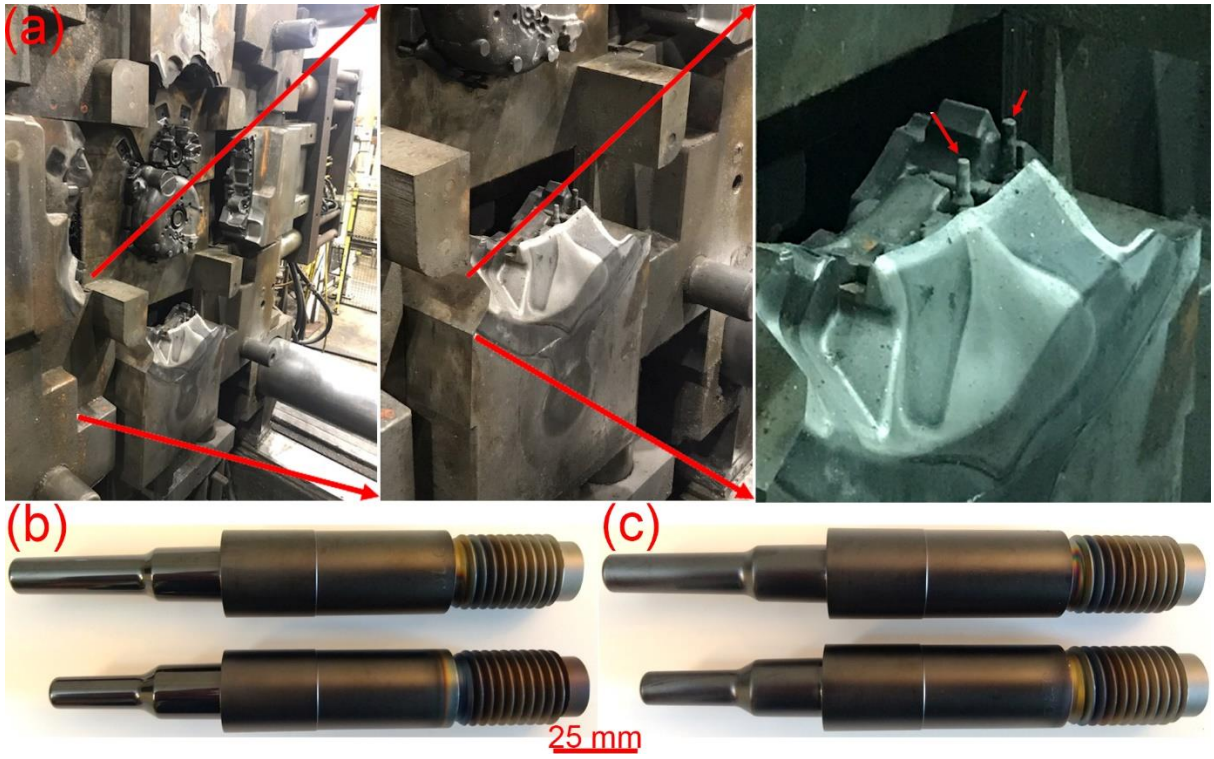

Figure 37.1: (a) Images of the die used for the soldering trial at Stellantis. Detail for the two core pins (models 5205 and 5215) located in front of the gate that received different PVD coatings with two surface finishes: (b) diamond polishing and (c) draw finish.

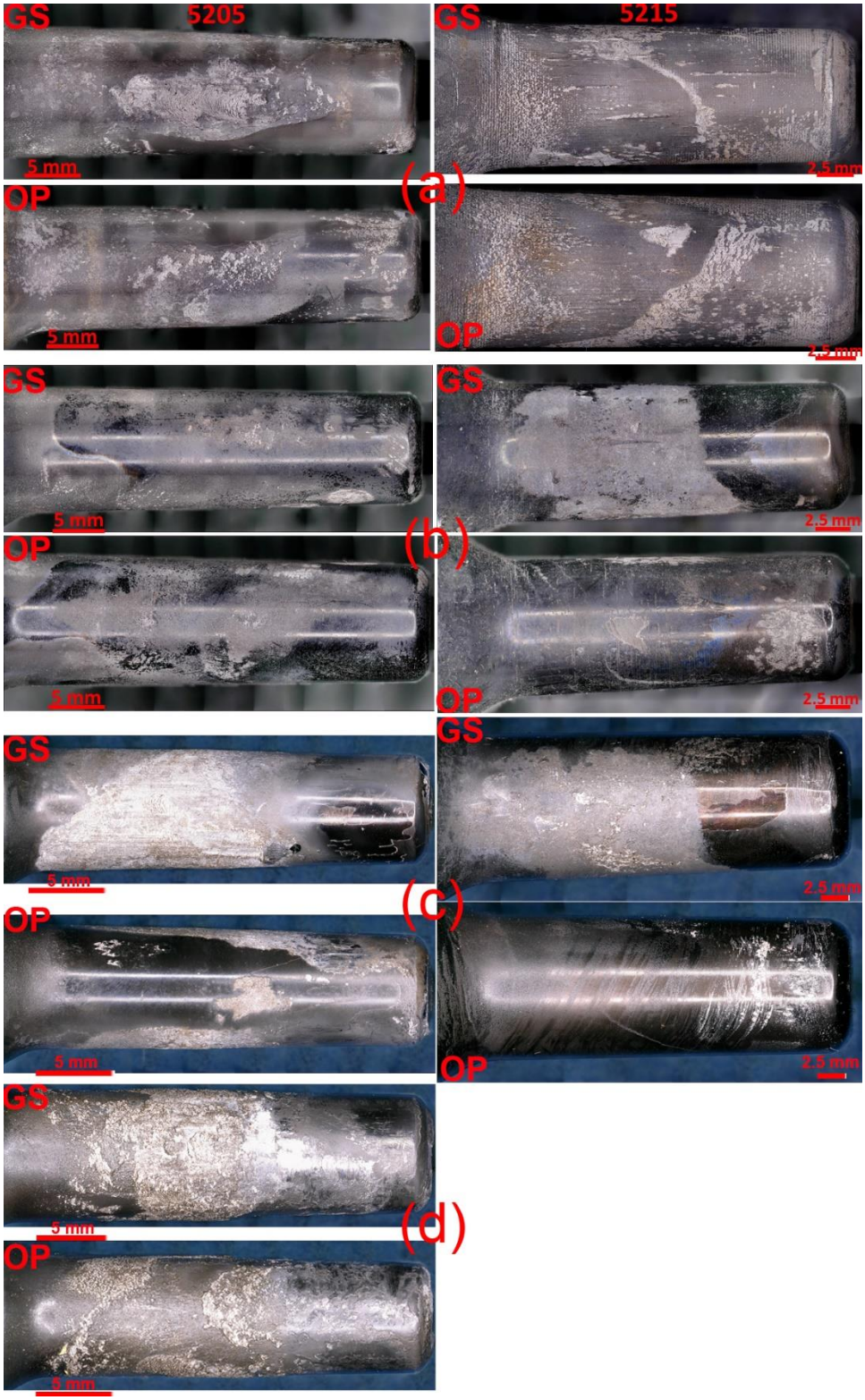

Figure 37.2: Optical 3D reconstruction for both sides of the surface of the tested core pins models 5205 and 5215, where: (a) nitride-draw, (b) Si-DLC-polished, (c) AlCrN/TiCN-polished, and (d) Al_2O_3-draw.

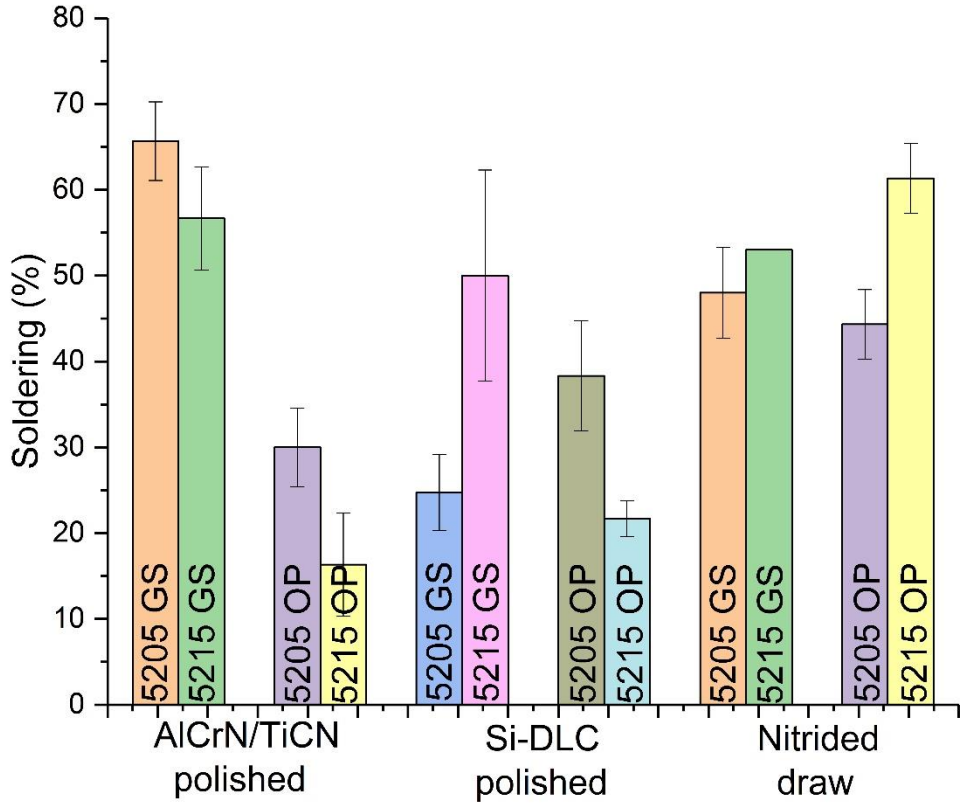

Figure 37.3: Soldering on different coatings comparing core pins models 5205 and 5215. GS = gate side, OP = opposite of gate side.

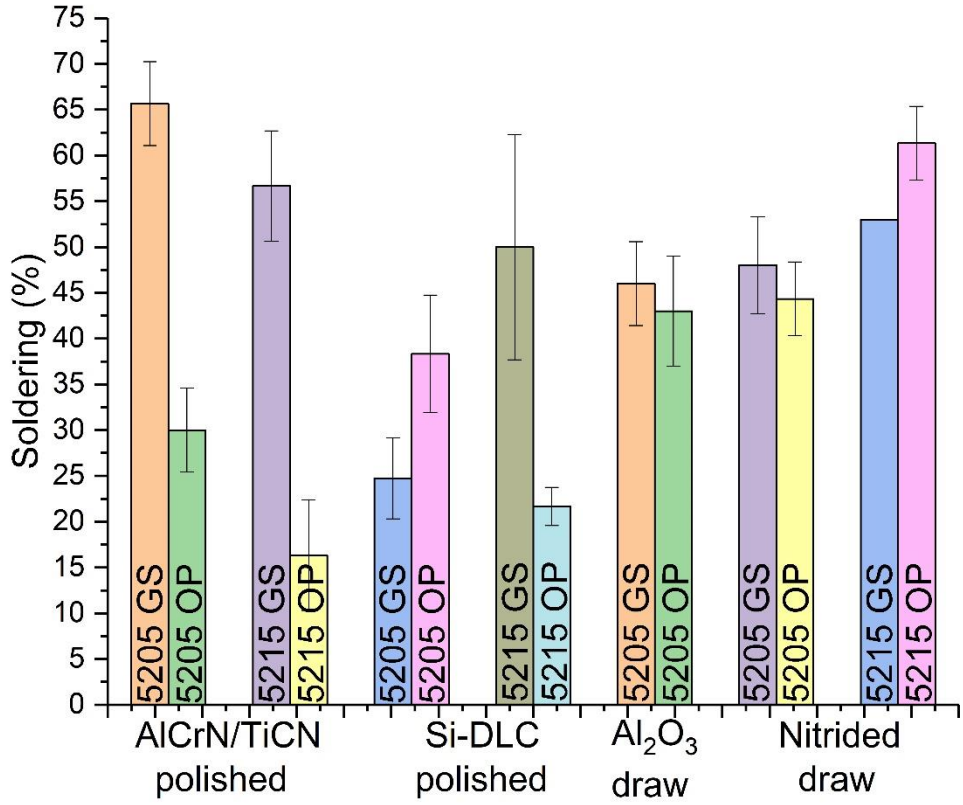

Figure 37.4: Soldering on different coatings comparing GS an OP sides for core pins models 5205 and 5215. GS = gate side, OP = opposite of gate side.

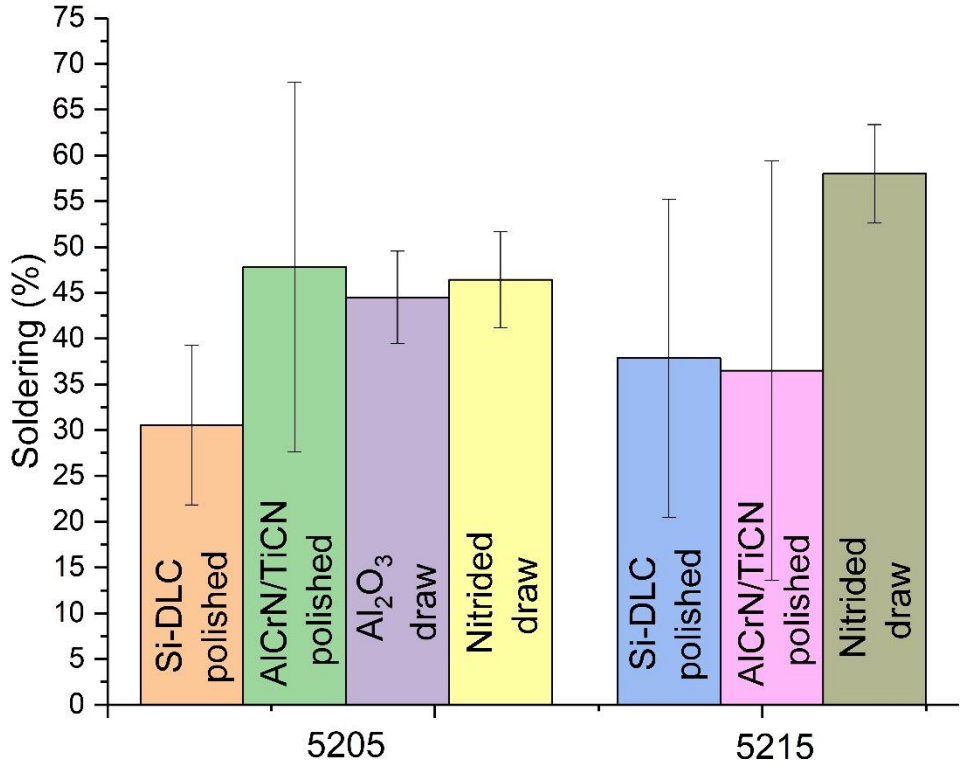

Figure 37.5: Average soldering on core pins 5205 and 5215 comparing different coatings performance.

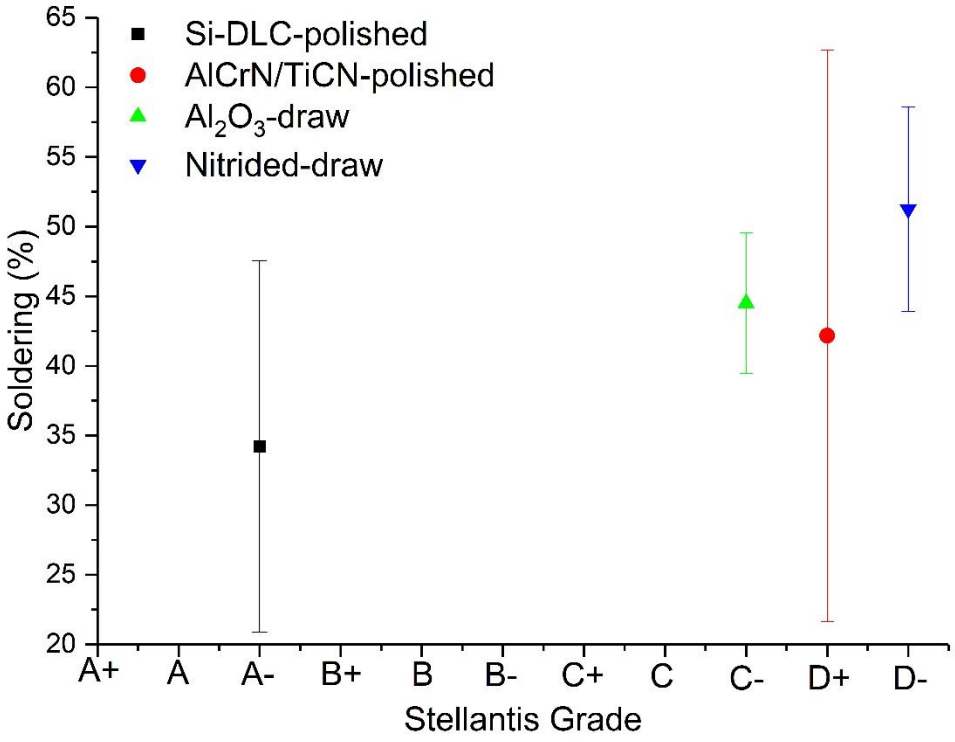

Figure 37.6: Correlation between the Stellantis grade (qualitative) and the measured soldering (quantitative) for different coatings performance.

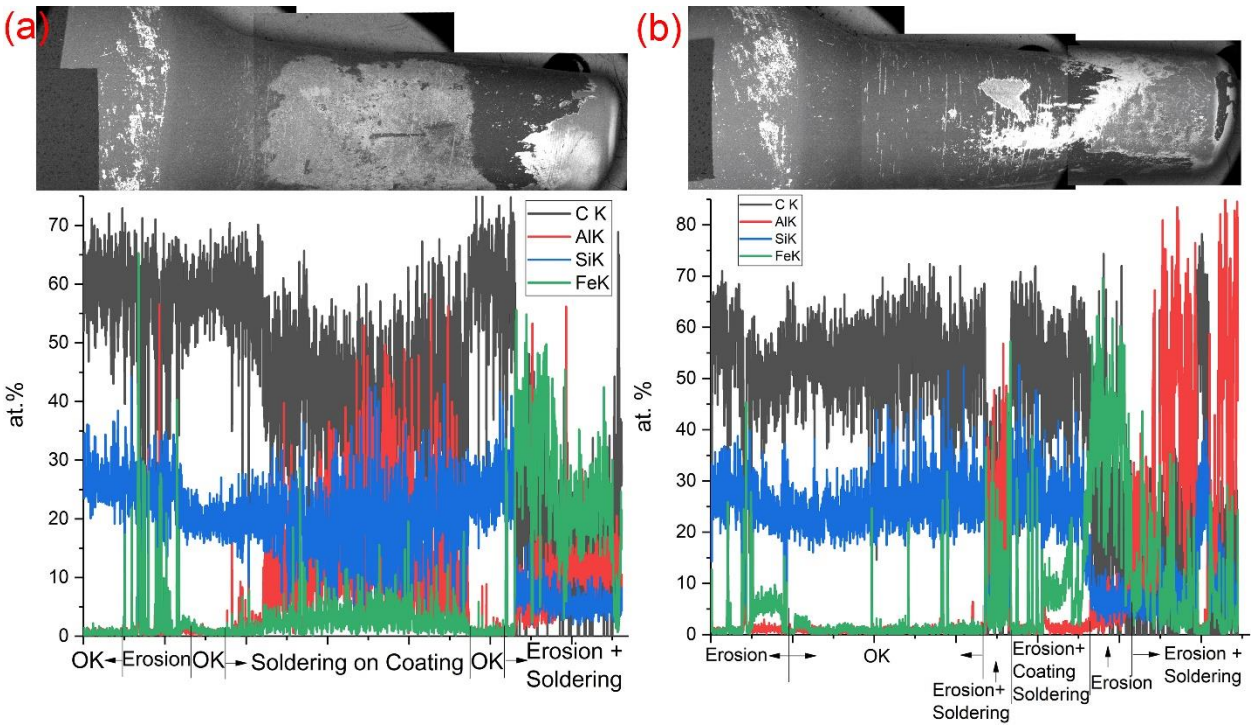

Figure 37.7: Back-scattered electron SEM image with EDS line scan of the Si-DLC-polished 5215 core pins, (a) GS and (b) OP side.

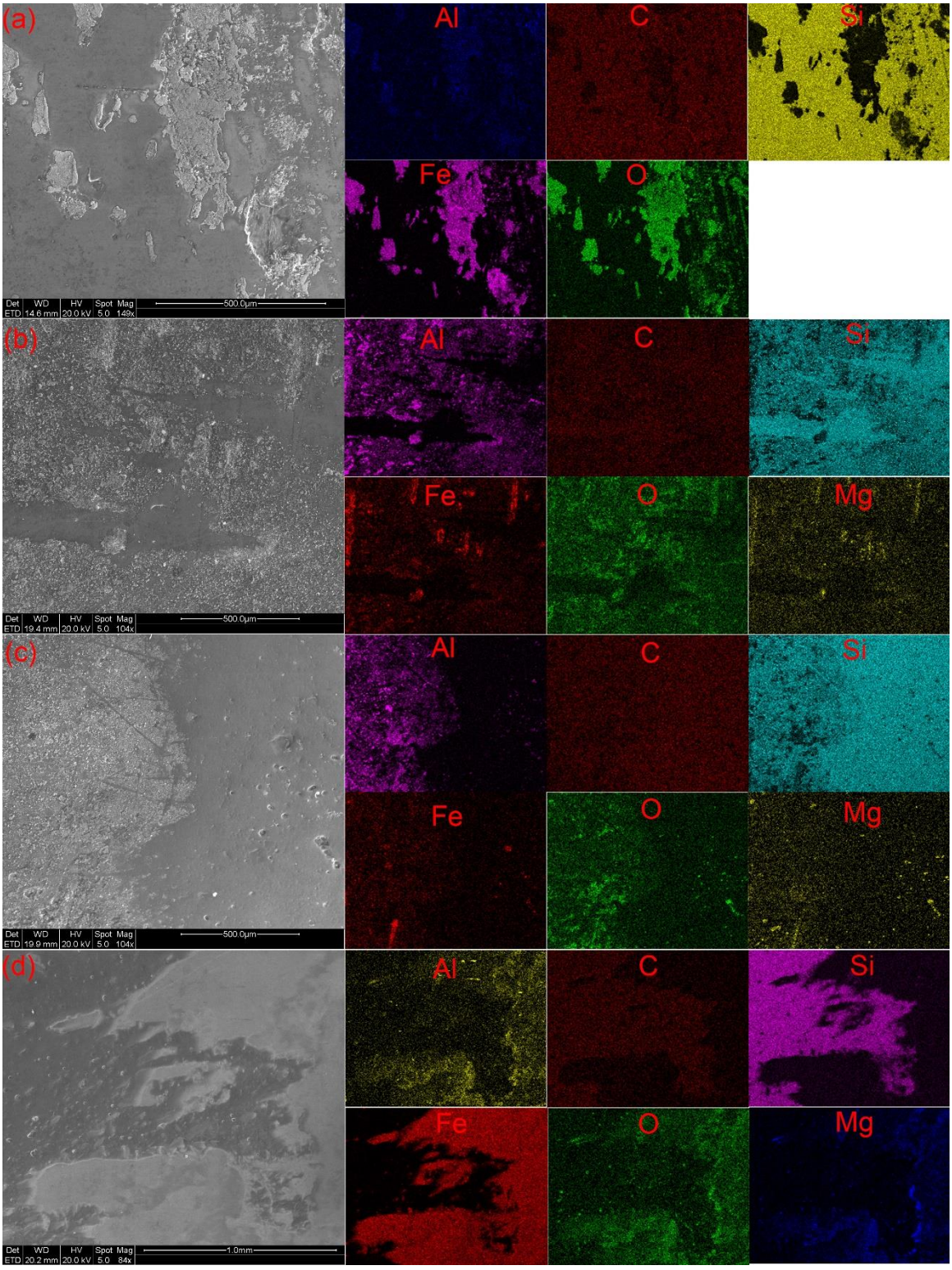

Figure 37.8: Secondary electron SEM image with EDS maps of Si-DLC-polished GS 5215 core pins for the different failure mechanisms, (a) erosion with minor soldering, (b) soldering on coating with minor erosion, (c) transition from soldering on coating to a coated region, and (d) erosion + soldering.

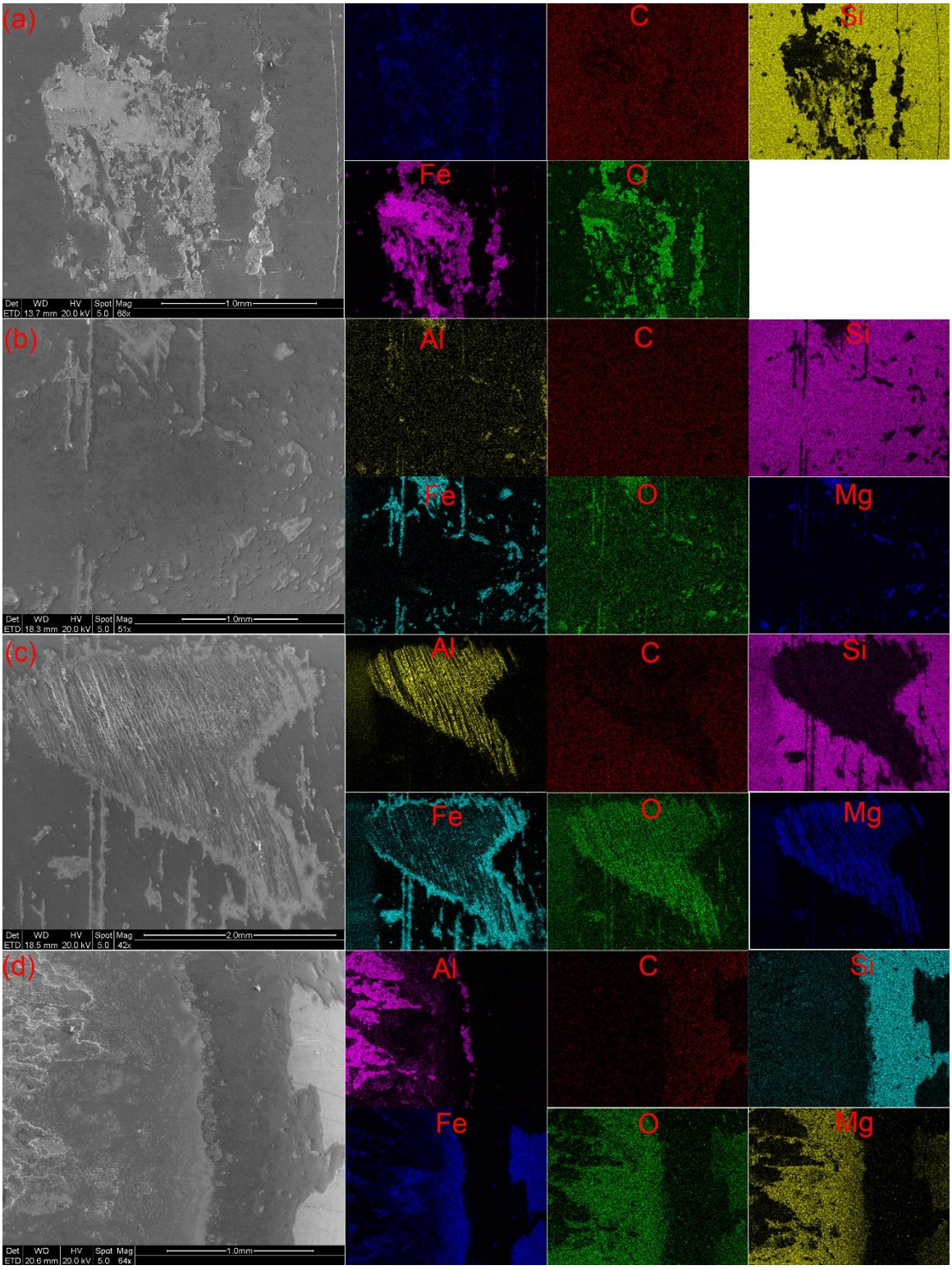

Figure 37.9: Secondary electron SEM image with EDS maps for Si-DLC-polished OP 5215 core pins for the different failure mechanisms, (a) erosion with minor soldering, (b) coated region (OK) with very minor soldering and minor erosion, (c) erosion and soldering, and (d) erosion + soldering up to the tip of the core pin.

Table 37.1: Results of the Stellantis test for the core pins model 5205 and 5215.

Coating	Coating Supplier	# of Shots	Stellantis Observations	Stellantis Grade	Mass change (5205) (g)	Mass change (5215) (g)	Soldering GS (5205) (%)	Soldering OP (5205) (%)	Soldering GS (5215) (%)	Soldering OP (5215) (%)
Nitrided - Draw	-	2500	Both cores soldered.	D	N/A	N/A	48 ± 5	44 ± 4	53 ± 1	61 ± 4
Si-DLC - Polished	#1	2430	Cores basically clean with no soldering. Soldering looks like it is intermittent.	A-	+ 0.20	+ 0.28	25 ± 4	38 ± 6	50 ± 12	22 ± 2
Si-DLC - Draw	#1	2503	Cores look clean. Note: core puller could have rubbed off some soldering).	B+	-	-	-	-	-	-
Al_2O_3 - Polished	#1	2572	Some soldering (cores got destroyed)	C+	N/A	N/A	N/A	N/A	N/A	N/A
Al_2O_3 - Draw	#1	3818	One core fairly clean, while the other had soldering on gate side. (one core got destroyed)	C-	+ 0.17	N/A	46 ± 5	43 ± 6	N/A	N/A
VC - Polished	#1	4469	Some light soldering (cores got destroyed)	B-	N/A	N/A	N/A	N/A	N/A	N/A
AlCrN/TiCN - Polished	#2	4112	One core relatively clean, while the other had soldering. Happening on gate side.	D+	+ 0.19	- 0.17	66 ± 5	30 ± 5	57 ± 6	16 ± 6